

See discussions, stats, and author profiles for this publication at: <https://www.researchgate.net/publication/318960214>

Understanding wave generation in pneumatic tsunami simulators

Conference Paper · May 2016

CITATIONS

3

READS

77

4 authors, including:



[William Allsop](#)

The University of Edinburgh

177 PUBLICATIONS 1,320 CITATIONS

[SEE PROFILE](#)



[Ignacio Barranco Granged](#)

National University of Singapore

2 PUBLICATIONS 3 CITATIONS

[SEE PROFILE](#)



[David John McGovern](#)

University College London

13 PUBLICATIONS 44 CITATIONS

[SEE PROFILE](#)

Some of the authors of this publication are also working on these related projects:



Impact wave-forces [View project](#)



Input to the Concrete Manual [View project](#)

UNDERSTANDING WAVE GENERATION IN PNEUMATIC TSUNAMI SIMULATORS

IAN D CHANDLER¹, WILLIAM H ALLSOP², IGNACIO BARRANCO GRANGED³, DAVID J MCGOVERN⁴

¹ HR Wallingford, UK, I.Chandler@hrwallingford.com

² HR Wallingford, UK, W.Allsop@hrwallingford.com

³ National University of Singapore, Singapore, i.barranco@u.nus.edu

⁴ University College London, UK, d.mcGovern@ucl.ac.uk

ABSTRACT

Tsunami crest only (elevated) and trough led N-waves have been generated using an improved pneumatic Tsunami Simulator. The crest only wave periods range from 20s to 160s, and 20s to 240s for the trough led N-waves. The length of flume in which these waves are generated was found to have an influence on the measured wave profile at a particular location for waves with period between 40s and approximately 120s. For waves less than 40s the wave generation is not affected by reflections. For waves greater than 120s the variation in free-surface elevation along the flume at any given instant is small resulting in negligible variation in measured profile from different positions within the flume. Outlines for further investigations and improvements to the Tsunami Simulator are given, including initial developments for an active wave absorption system for the Tsunami Simulator.

KEYWORDS: Tsunami, Physical modelling, Tsunami Simulator, Wave generation

1 INTRODUCTION

Tsunamis are very long-period (10-30 minute) waves caused by sub-marine seabed movement or terrestrial landslides impacting a body of water. They are a relatively rare, yet often extremely destructive. As examples the 2011 Tohoku Tsunami and the 2004 Indian Ocean (Boxing day) Tsunami together caused the loss of approximately 300,000 lives and caused billions of dollars of economic and infrastructure losses (e.g. Kajitani *et al.* 2013). A notable feature of some tsunamis, particularly those on the ‘upward’ side of a subduction zone, is the initial depression or trough that precedes the main wave crest. Historically the majority of physical experiments worldwide have been limited to generation of solitary waves as an approximation for tsunami. Madsen *et al* (2008) have however demonstrated that solitary waves do not represent realistic tsunamis. The move in recent years has been to use N-waves or to recreate measured time series from specific tsunami events (e.g. Rossetto *et al.*, 2011, Allsop *et al.*, 2014a and 2014b, and Schimmels *et al.*, 2014).

Experimental data of long waves is relatively rare, primarily due to the complexities of reproducing long period waves, in laboratories. Tsunami period waves, even at small / moderate model scales, have wavelengths in the hundreds of metres. This requires long flumes to accommodate representative free-surface elevation characteristics before reflections interfere with the measured signal. Furthermore it is difficult to generate very long wavelengths with traditional piston type wave makers where the stroke limits the wavelengths and amplitude that can be generated. Schimmels *et al* (2014) demonstrated some success with a piston type wave maker, but scales were 1:100 at best and the reproduction of the leading troughs was not as clean as that of the crest generation, suggesting that the trough generation may not be as stable.

A novel pneumatic Tsunami Simulator (TS) was developed by HR Wallingford with the support of University College London (UCL) in 2008 and has been used to study tsunami and their effects on run-up and buildings, Allsop *et al* (2008, 2014a and 2014b), Rossetto *et al* (2011) and Charvet (2011, 2013). The pneumatic TS can generate both crest and trough led waves as well as reproduce measured tsunami time signals such as that from the Mercator yacht during the 2004 Indian Ocean Tsunami. A second generation TS has been constructed by HR Wallingford as part of the URBANWAVES project (ERC grant no. 336084). Through this work the mechanism for wave generation using the pneumatic TS has been explored and better understood. This paper will focus on the effect flume length and wave reflections have on the wave generation.

2 BACKGROUND

2.1 TSUNAMI SIGNALS

The input wave signal has a significant impact of the results obtained from physical modelling. A number of different wave forms have been used to characterize tsunami in physical model experiments. These range from generic signals such as solitary or N-waves, to reproducing measured tsunami time series. One of the most common wave signals used historically to describe tsunami is the solitary wave, or soliton. This is a shallow water wave which consist of a single positive displacement (crest) of water above the mean water level.

2.1.1 SOLITARY AND N-WAVES

Hammack (1972) showed how a positive initial surface disturbance will eventually decompose into solitons, and this conclusion has been used to justify the use of solitons to model tsunamis (Allsop *et al*, 2014a). Madsen *et al* (2008) argued that the assumptions this solution implies may not be relevant to earthquake induced geophysical tsunamis.

Tadepalli & Synolakis (1994) proposed replacing the solitary wave with an N-shaped solitary-like wave, which can be either a leading depression N-waves (LDN) or a leading elevation N-waves (LEN). The generalized N-wave is given by:

$$\eta(x, 0) = \alpha H(x - x_2) \operatorname{sech}^2(k(x - x_1)) \quad (1)$$

Where η is the free-surface elevation, $k = 1/h \sqrt{(3H/4h)}$, H is crest amplitude, h is local water depth, α is a scaling parameter to allow comparison with solitary waves and x_1 and x_2 define the locations of trough and crest..

Their work was qualitatively supported by accounts of wave recession before the arrival of the tsunami wave in Indonesia 1992, Nicaragua 1992 and Philippines 1994. This phenomenon has also been observed in the Mexico 1995, tsunami and in Thailand in 2004. Tadepalli & Synolakis (1994) suggested that the nature of the sea floor deformation in subduction zones leads to LDN waves on the subsiding plate, whereas LEN waves travel away from the sub-duction zone towards the open ocean. They also found that N-waves with a trough-led (LDN) run-up higher than crest-led N-waves (LEN). They report that LEN waves nevertheless have higher run-ups than their equivalent solitary waves.

2.1.2 TIME SERIES

An inherently more realistic option is to base a simulation on an incident wave as recorded during a known tsunami event. Ideally, a clean signal should be obtained in a nearshore area, and on the direct trajectory of the tsunami, and to avoid noise and distortion due to local effects and reflections (Allsop *et al*, 2014a). Achieving this has proved extremely challenging.

The 2004 Indian Ocean tsunami has produced one of the best time series obtained from a tsunami, the 'Mercator' signal. It is the closest signal to a generic recording of the 2004 Indian Ocean Tsunami. The 'Mercator' signal was recorded by a Belgian yacht of the same name anchored 1.6km off the coast of Phuket (Thailand). The boat rode the tsunami wave with its depth-sounder recording continuously. The depth-sounder recorded the depth variation during the tsunami giving a record of the local depth, which, when inverted, gives the surface elevation.

The time series recorded by the Mercator is shown in Figure 1. The time series was trough-led (-2.77m) and includes several following peaks, although these further oscillations may be strongly influenced by reflections from the shoreline. Because the later part of the signal is likely to be reflections from the shoreline, only the first part of the signal has been used in experimental studies (e.g. Rossetto *et al*, 2011 and Schimmels *et al*, 2014). The parameters of the main wave (respectively: wave height, crest amplitude, trough amplitude and wavelength) are the following: $H=6.5\text{m}$, $a_{\text{crest}}=3.7\text{m}$, $a_{\text{trough}}=2.8\text{m}$, and $L=14400\text{m}$, Rossetto *et al* (2011).

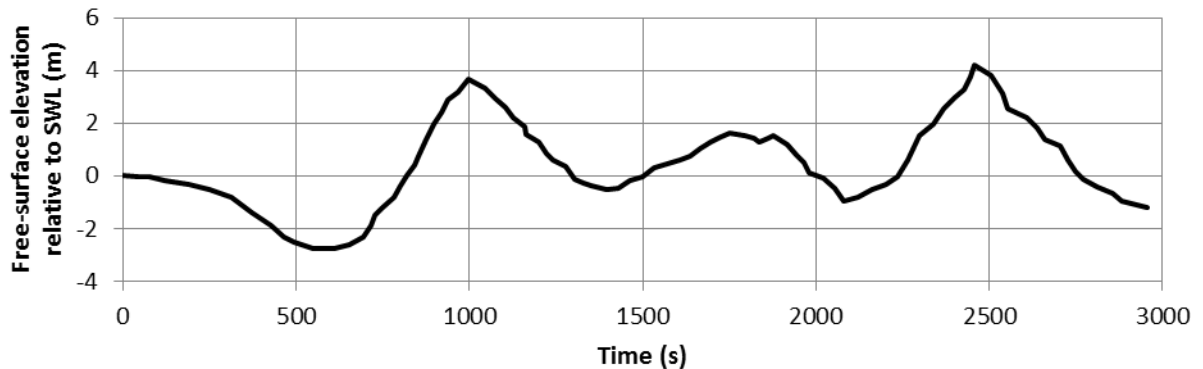


Figure 1 Signal recorded by the Mercator yacht during 2004 Indian Ocean tsunami.

2.2 PNUMATIC TSUNAMI SIMULATOR

The principles of the pneumatic TS are based on those for a physical model tidal generator (Wilkie & Young, 1952). The system works by creating a vacuum within a steel box which has an outlet below the free-surface in the flume. In the second generation TS two Zepher^{UK} vacuum pumps are used to draw air continuously out of the TS. A computer controlled 45° butterfly air valve is used to control the relative vacuum and hence the water level inside the TS, termed tank water level (TWL). Raising the TWL creates a depression in the free-surface in the flume, creating a wave trough. Lowering the TWL increases the flume water level creating a wave crest. This process is shown in Figure 2.

Details of the first generation TS are given in several papers, Allsop *et al* (2008), Rossetto *et al* (2011) and Charvet (2011). Both solitary and N-waves were generated with periods ranging from 5.5s to 18.0s. The outlet of the first generation TS was improved through the work reported by Allsop *et al* (2014a, 2014b) including the addition of a flow shaper to the outlet to reduce turbulence as the wave is generated. This work culminated with the reproduction of the Mercator time series at a model scale of 1:50 (Figure 3).

The main improvements for the second generation TS are a change from a 45m long by 1.2m wide flume to a 100m long by 1.8m wide facility. This has implications for the wave generation that will be explored later in this paper, but has also increased the range of processes / structures that may be tested in the wider flume.

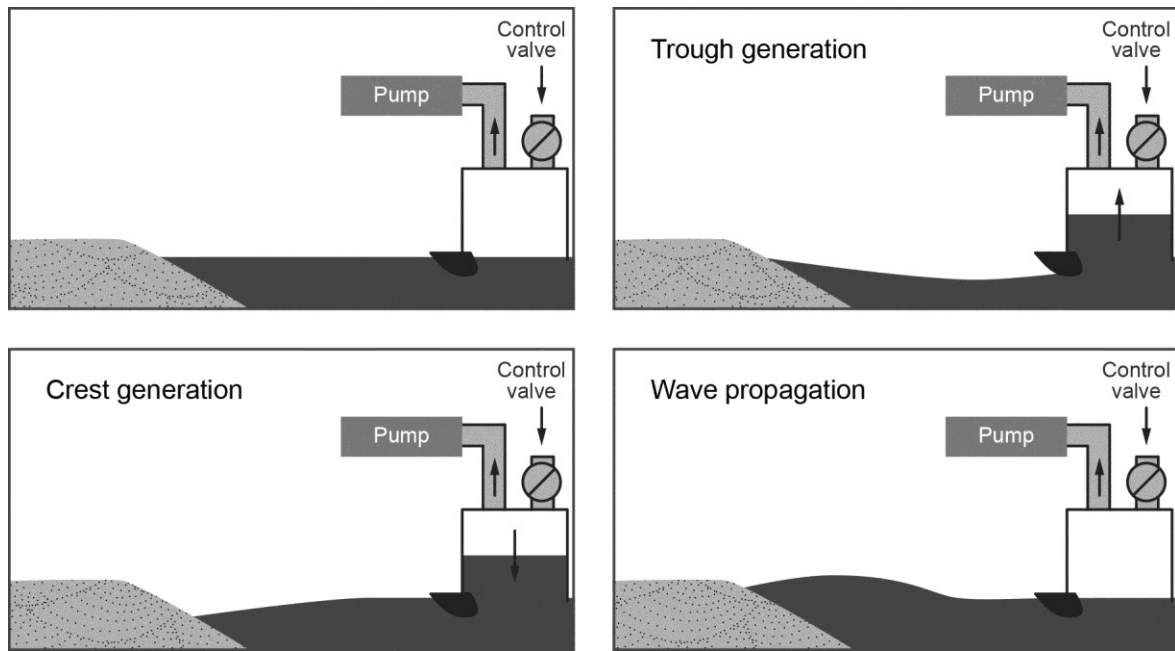


Figure 2 Schematic diagram of pneumatic Tsunami Simulator.

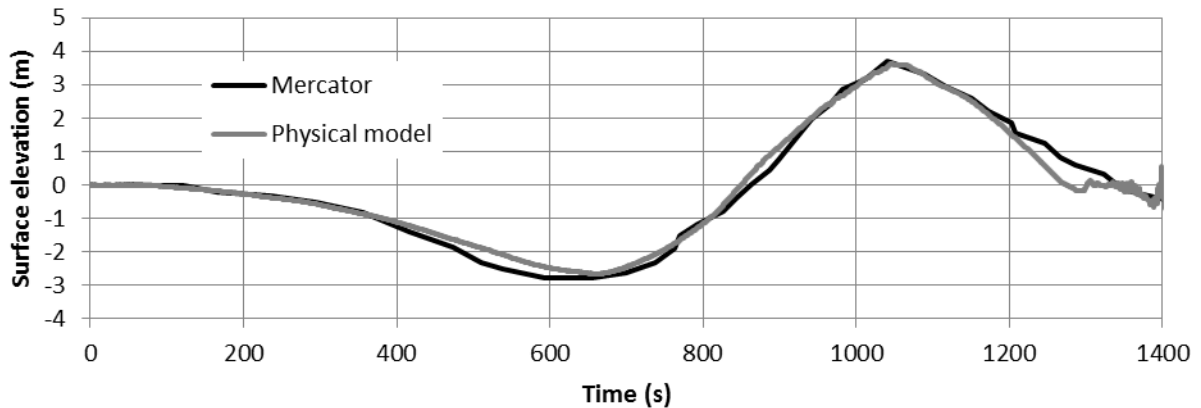


Figure 3 Reproduction of Mercator time series at 1:50 scale with 1st generation Tsunami Simulator.

The safety valve used in the 1st generation TS has been replaced by an electrical float switch and the generation software has been improved, making it more user friendly. The control system for the air valve has also been improved and now uses the Beckhoff EtherCAT system which also extends to all of the IO, pump control and safety systems. A second, more powerful vacuum pump has been added which has allowed the second generation TS to be almost twice as tall as the first generation. The TS tank dimensions are now 4m long, 1.8m wide and 3.5m high. The TS tank is instrumented with two ultrasonic water level sensors measuring the TWL, and a pressure transducer fitted to the back of the TS, 0.2m above the base of the tank (at the bed of the flume).

3 EXPERIMENTAL SETUP

A schematic diagram of the experimental setup used with the 2nd generation TS is shown in Figure 4. The ‘offshore’ region of the flume is 65.6m long with a 1.0m high bathymetry comprising of a 1:20 approach slope and a 5.0m horizontal area. A sump was created to catch overflow water and prevent unrealistic reflections from the end of the flume should overflow occur. During wave calibrations a vertical sea-wall was present at the crest of the 1:20 slope, preventing water from running up and over the horizontal area and into the sump (overflow). The wall was high enough to prevent overtopping (overflow) of all the waves presented in this paper.

All horizontal (x) distances are taken from the front wall of the TS. Six twin wire resistance based wave gauges were placed at intervals along the flume and on the bathymetry to measure free-surface elevation. The positions of the gauges are given in Table 1 along with the still water level at each position. The free-surface elevation was recorded at a sampling rate of 100Hz using HR Wallingford’s HR DAQ software (HR Wallingford, 2013). The data acquisition was triggered from the TS wave generation software enabling time coincident measurements to be recorded in the flume and from the TS.

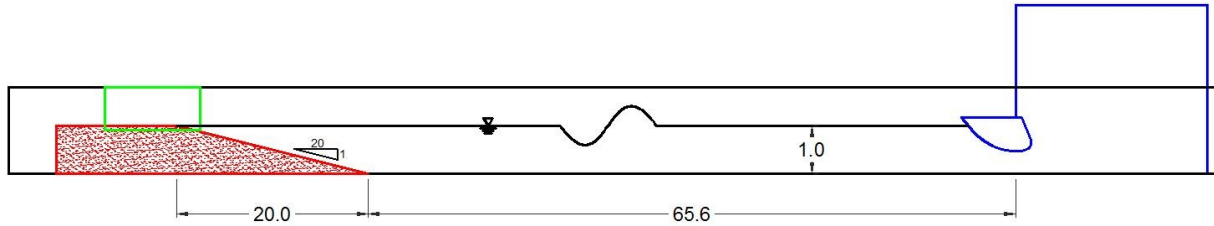


Figure 4 Schematic of 2nd generation Tsunami Simulator setup showing the Tsunami Simulator with the flow shaper at the outlet, bathymetry and window position.

Table 1. Wave gauge position measured from the front of the TS

Name	Distance from TS (m)	Water depth, h (m)
WG_01	7.0	1.0
WG_02	12.0	1.0
WG_03	17.0	1.0
WG_04	22.0	1.0
WG_05	65.6	1.0
WG_06	75.6	0.5

4 WAVE GENERATION

The basic principle of wave generation is described in Section 2.2. There are however several factors that influence the wave generated which depend on the geometry of the generator and of the flume. The construction of the 2nd generation TS through the URBANWAVES grant has allowed these factors to be investigated.

Two families of waves (elevated or crest only, and N-waves) have been calibrated using the second generation TS. The point of calibration was chosen to be the toe of the 1:20 slope, wave gauge position WG_05. The calibration of the waves was an iterative process with the air valve time series adjusted manually based on the generated wave profile.

4.1 INFLUENCE OF FLUME GEOMETRY

The geometry of the flume has an impact on the waves generated within it. All the waves presented in this paper can be assumed to be shallow water waves, therefore the celerity of the waves can be estimated using the shallow water approximation. For a water depth of 1.0m the wave celerity (c) should be approximately $c = \sqrt{gh} = 3.13\text{m/s}$. The distance between the front of the TS and the toe of the bathymetry is 65.6m (Figure 4). Allowing for the fact that reflections will occur over the length of the 1:20 slope this results in a ‘reflection length’ of approximately 70.0m.

Using this length and the assumed celerity, a 22s wave will have finished generation before any natural reflections

from the bathymetry have occurred. A wave with a 45s period will have finished generation before the natural reflections reach the TS. Waves longer than 45s will be subject to interference from ‘false’ re-reflections from the TS which will propagate back along the flume with the generated wave. The re-reflection from the TS can be assumed to be 100% unless the valve time series is manually adjusted to compensate and absorb the natural reflection from the bathymetry. The reflection coefficient from the bathymetry and vertical wall present at the top of the 1:20 slope has been estimated to be about 67% based on incident and reflected elevated wave amplitudes.

The natural period of resonance of the flume can have an influence on the generated waves, particularly for those longer than the length of the flume. The natural seiching period as calculated using Merian's formula ($T = 2L/\sqrt{gh}$) (as given by Rabinovich in Kim, 2010) is 44.7s. The second harmonic is 22.3s and this will be shown to be more influential than the first harmonic during wave generation.

4.2 CREST ONLY (ELEVATED) WAVES

The calibrated family of four different period crest only (elevated) waves is shown in Figure 5 and demonstrate the second generation TS’s ability to generate solitary like waves, with no free-surface variation preceding the wave. The main parameters for the calibrated crest only waves are given in Table 2. The elevated waves are close to the maximum possible amplitude achievable with the 2nd generation TS at each period. Because the generator has a finite capacity, the longer a wave period, the smaller the amplitude achievable as the available volume inside the TS is spread over a longer time.

The variation in free-surface elevation visible at the start of the 160s period wave (Figure 5) is due to residual seiching in the flume from the generation of a previous wave. This seiching continues to have an influence on the generated wave profile throughout the generation and shows the importance of leaving enough time between wave generations to allow the previous wave to dissipate. Without using specific damping, this process was found to take between 20 and 30 minutes.

For shorter period waves the propagation of the waves can be tracked along the flume. Figure 6 shows the propagation of a 20s elevated wave. The wave is unchanged as it propagates over the area of constant depth (‘offshore’ region), and then shoals when it reaches the 1:20 slope (WG_05 and 06). The reflection from the vertical wall at the top of the 1:20 slope can be seen in the second half of WG_06 and then travelling back down the flume to WG_05, arriving at approximately 45s. The wave fissions as it propagates against the continued arrival of the incident wave.

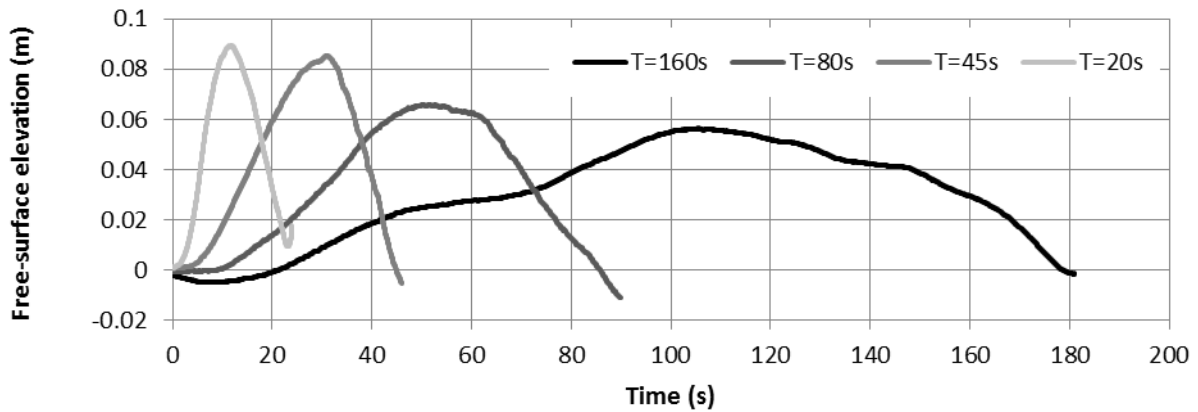


Figure 5 Calibrated crest only (elevated) waves using second generation TS, measured at the toe of the bathymetry (WG_05).

Table 2. Calibrated crest only (elevated) waves using second generation TS

Name	Period, T (s)	Crest amplitude, A_c (m)	Calculated wave length, λ (m)
Elevated_T=160s	160	0.056	501
Elevated_T=80s	80	0.066	251
Elevated_T=45s	45	0.085	141
Elevated T=20s	20	0.089	63

Note: Wave length calculated using the shallow water approximation

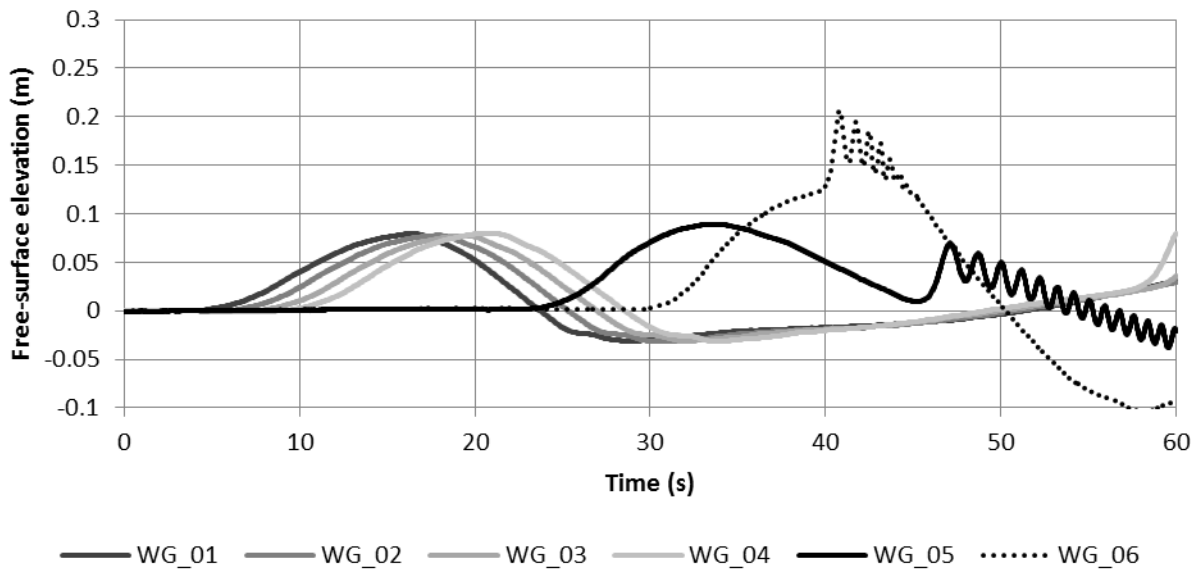


Figure 6 $T = 20s$ elevated wave propagating along flume, WG_01 to 04 in constant depth, WG_05 at the toe of the 1:20 slope and WG_06 on the 1:20 slope.

4.3 N-WAVES

The family of calibrated N-waves is shown in Figure 7, and a summary of their parameters is given in Table 3. The periods range from 20 to 240s, with the majority calibrated to an amplitude of 0.04m. This was to allow the influence of wave period only on run-up (McGovern *et al.*, 2016), and to measure their impact on coastal structures, to be studied later in the URBANWAVES research programme. Two waves were calibrated at close to the limit of the 2nd generation TS and are labeled 'max' indicating maximum amplitude. The longer period waves are also at the maximum achievable by the TS and the 0.04m wave amplitude was based on that achievable for the 240s period N-wave.

The influence of both reflections and seiching can be seen in the calibrated N-waves (Figure 7). The position of the calibration wave gauge influences the measured surface elevation profile of the 40s period wave. The falling edge of the crest is disrupted by the reflection of the preceding part of the wave from the vertical sea wall present at the crest of the 1:20 slope. The traces from the preceding wave gauges (WG_01 to 04) show the clean generation of this period N-wave (Figure 8) in the 'offshore' region and confirm that the free-surface elevation measured at the calibration point is influenced by reflections and not a function of the wave generation. There is also some indication that at the chosen calibration point the wave has started to shoal. This is possibly due to bottom friction along the flume rather than a change in slope (which has not been 'felt' by the wave at this point) and which causes a more dramatic change to the wave between WG_05 and 06. Constructive interference from natural reflections from the bathymetry may also account for an increase in amplitude at the calibration point for certain wave periods.

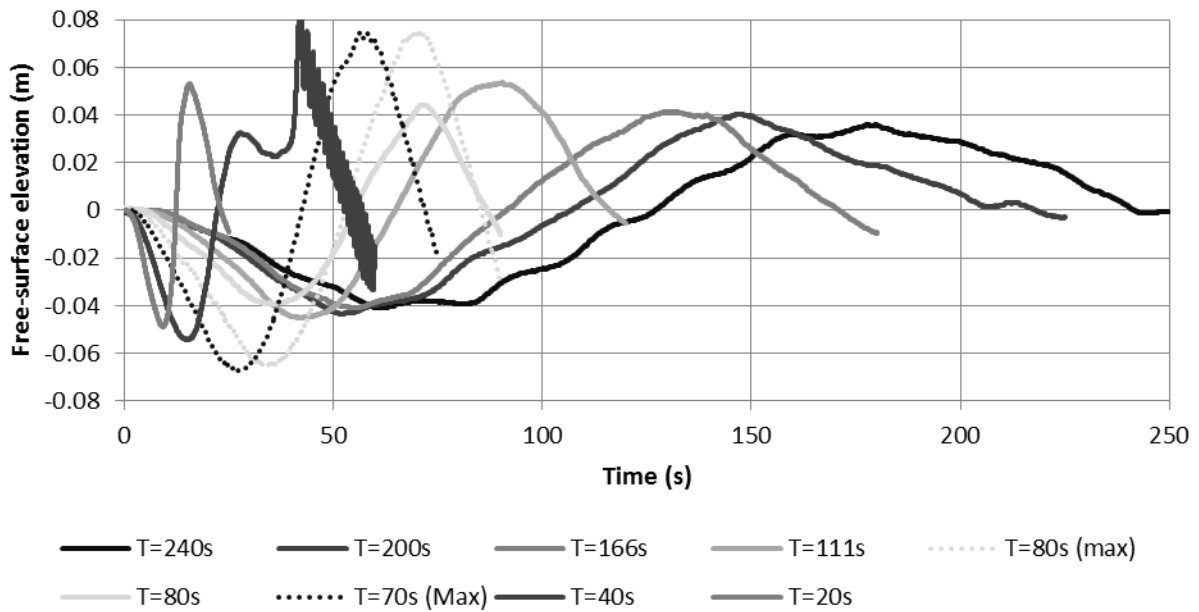


Figure 7 Calibrated N-waves using 2nd generation TS, measured at the toe of the bathymetry (WG_05).

Table 3. Calibrated N-waves using 2nd generation TS

Name	Period, T (s)	Crest amplitude, A_c (m)	Trough amplitude, A_t (m)	Calculated wave length, λ (m)
Nwave_T=240s	240	0.036	-0.041	752
Nwave_T=200s	200	0.040	-0.043	626
Nwave_T=166s	166	0.041	-0.041	520
Nwave_T=111s	111	0.053	-0.045	348
Nwave_T=80s	80	0.044	-0.039	251
Nwave_T=80s_max	80	0.075	-0.065	251
Nwave_T=70s_max	70	0.075	-0.067	219
Nwave_T=40s	40	0.033	-0.054	125
Nwave_T=20s	20	0.053	-0.049	63

Note: Wave length calculated using the shallow water approximation

The influence of reflections on long period waves is shown in the 240s period N-wave (Figure 7), reproduced with the other wave gauge positions in Figure 9. A periodic oscillation can be seen superimposed on the underlying N-wave. If the main N-wave is removed from the time series the periodic oscillation in the flume becomes clear. This is shown in Figure 10 along with a 22s period sine wave, representing the second harmonic of the natural period of the flume as discussed in Section 4.1. There is very good agreement between the 22s sine wave and the periodic oscillation superimposed on the 240s N-wave. This seiche does not appear to significantly influence the generated wave, however it would be desirable to remove this from the generated wave if possible.

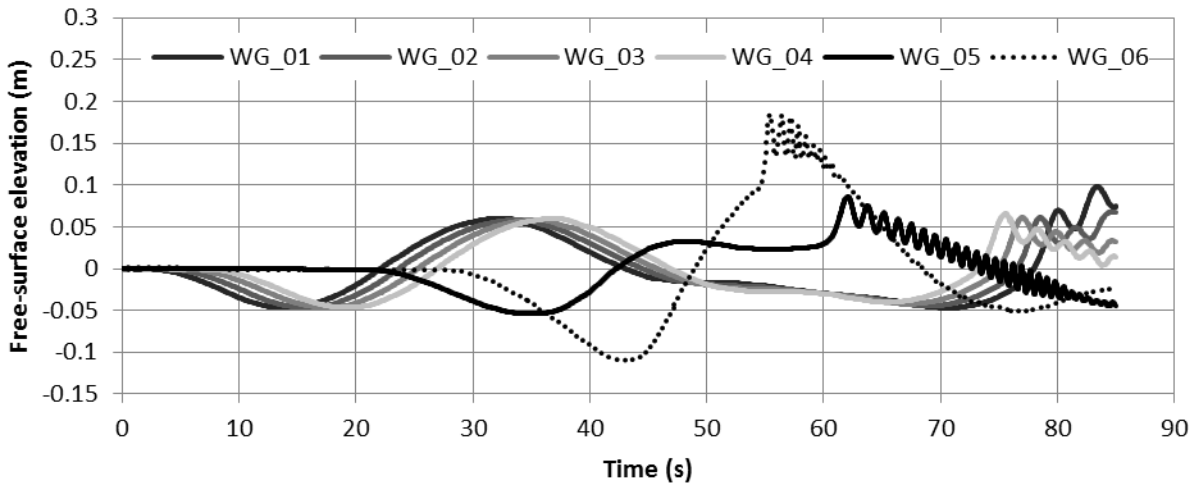


Figure 8 Influence of wave gauge position on measured free-surface elevation for $T=40s$ N-wave.

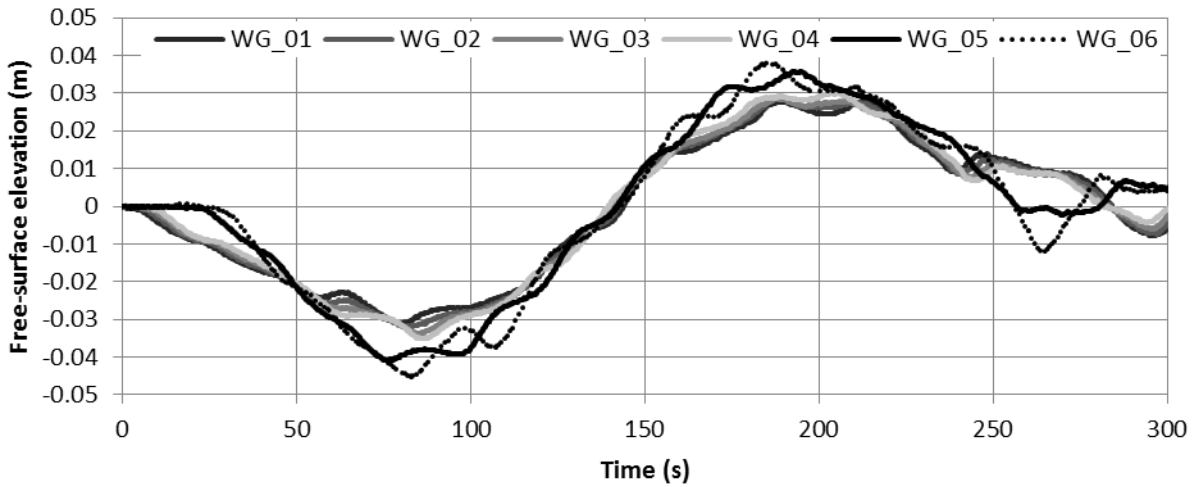


Figure 9 Surface elevation from all wave gauges for the 240s N-wave showing interference from reflections.

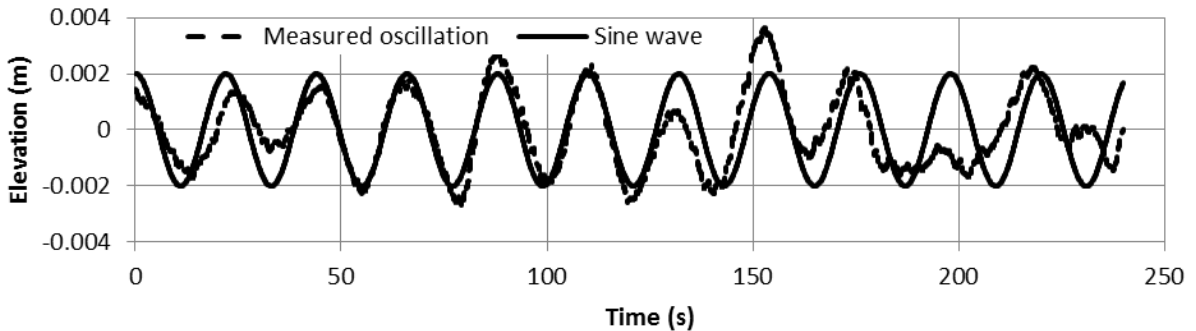


Figure 10 Periodic oscillation in the flume during 240s N-wave generation (dashed line) and a 22s period sine wave (solid line).

4.4 DISCUSSION

The presence of reflections from the bathymetry for a generated wave is to be expected and is a natural process. The re-reflections from the TS and seiches within the flume are model effect and are less-desirable. These do not appear to have significantly affected the waves generated by the 2nd generation TS, but the removal of them would alleviate any doubt and would reduce the time required between tests waiting for the flume to settle.

To achieve this we are developing an active absorption system for the TS, similar to that seen in several paddle / piston

type wave maker systems or that employed by Goseberg et al. (2013). The initial concept was to use the tank water level (TWL) as the monitored parameter to control the proportional-integral-derivative (PID) feedback system. The valve angle would be automatically adjusted to create the desired TWL at any given instant in time. Initial work has demonstrated that the TWL is not sensitive enough to the reflected wave to allow it to be used as the feedback parameter. Using the 40s N-wave as an example, the valve angle is plotted with the TWL, pressure measured at the base of the TS and the free-surface elevation at the first wave gauge (Figure 11). The noise in the TWL signal during crest generation ($t = 80$ s) is caused by condensation forming on the head of the ultrasonic depth gauge due to the change in pressure within the TS, giving intermittent false readings. The general trend within the signal is however still clear.

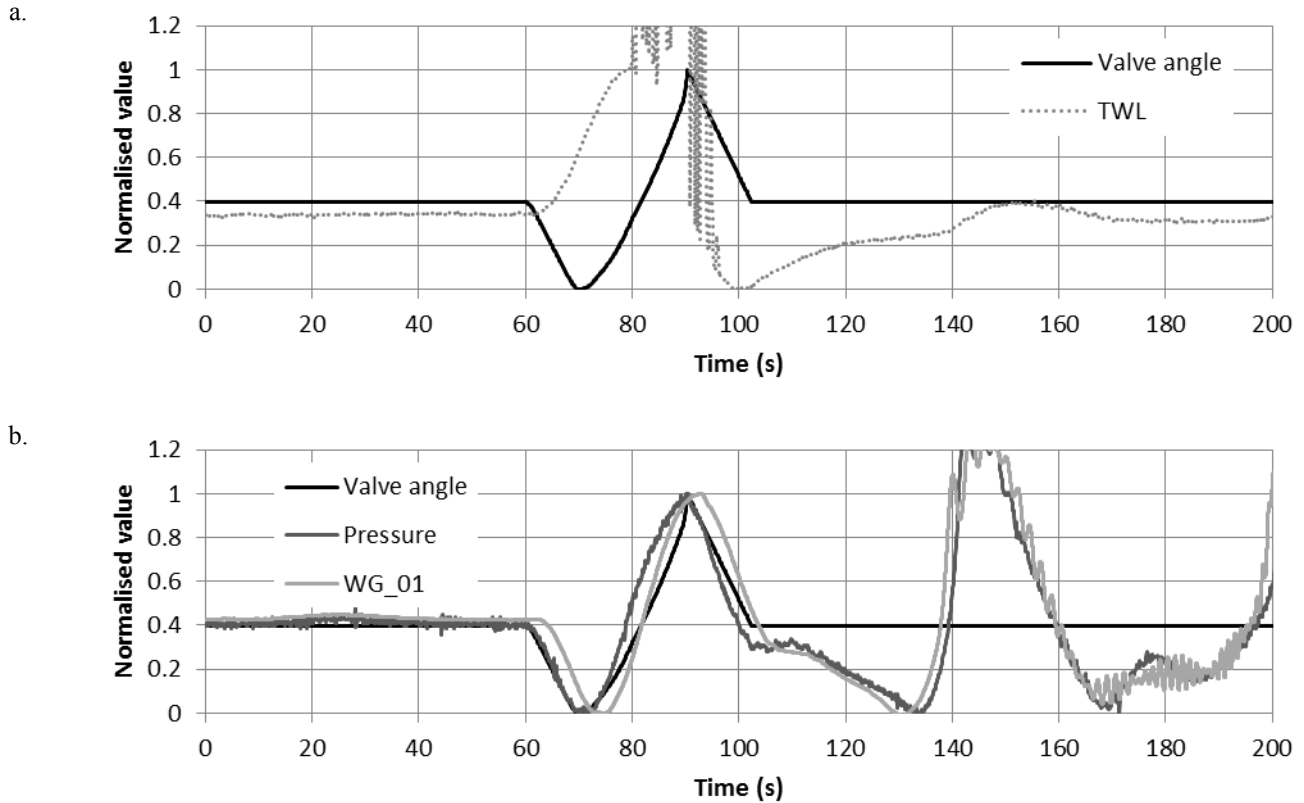


Figure 11 Normalised valve time series with the normalised TWL (a) and normalised valve time series with tank pressure transducer and WG_01 free-surface elevation (b) for $T=40$ s N-wave. All normalised using the primary peak and trough of the signal, ignoring additional reflections

There is a much stronger relationship between the valve angle and the signal from the pressure at the base of the TS, and the free-surface elevation measured at WG_01. This is further demonstrated in Figure 12 where the time coincident values are plotted against each other. Further development is needed on the active absorption system for the TS, however the strong correlation between the pressure at the bottom of the TS and the valve angle when in motion suggests this is a promising variable to base the feedback system on. A parameter within the TS is preferable to basing the feedback on rather than a wave gauge in front of the TS as there is a travel time between the two which would have to be accounted for in any feedback system. Additionally the direction of a wave cannot be determined from a single point measurement of free-surface elevation so it would not be possible to assign the correct positive or negative time correction for the valve movement within a feedback system. This is similar to the findings of Goseberg et al. (2013) who based their PID control on a pressure sensor situated within the flume.

To some extent false re-reflections from the TS have already been accounted for in the generation of the calibrated waves. If a reflected trough coincides with the generation of a wave crest, then to achieve the correct wave amplitude the crest will have been over-generated relative to a crest of the same amplitude generated at still water level. This process has occurred manually to date and is therefore imperfect in dealing with all reflections.

The presence of reflections and their influence on the measured wave profile demonstrates the importance of choosing a calibration point within the flume. This is of particular importance for waves that are longer than the flume as the measured profile will change at the different wave gauge positions within the flume. There is a transition region where the position of calibration has a significant impact on the waveform measured which, for the second generation TS, appears to be between 40s and 120s wave periods. For waves much longer than the flume, e.g. the 240s N-wave, the position of

calibration within the flume becomes less critical. This is because the generated wave is acting more like a tide within the flume, where the free-surface variation along the length of the flume at any instant in time is small, therefore the signal is very similar at all wave gauges (Figure 9). This was the case for the majority of waves generated using the first generation TS in a 40m flume (reflection length approximately 20m when the bathymetry present during the experiments is accounted for). It may be advisable in future calibrations to use a combination of wave gauge positions to determine the wave parameters in the ‘offshore’ region between the TS and the toe of the bathymetry.

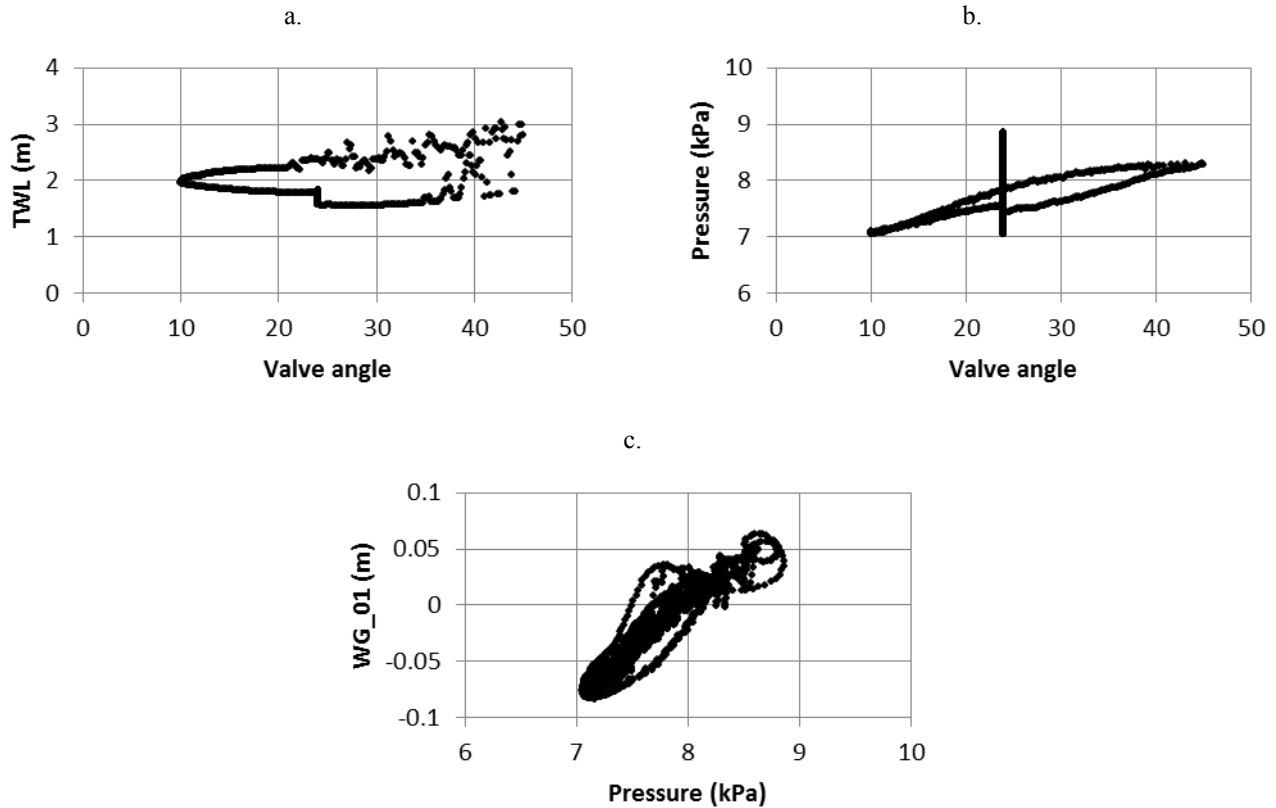


Figure 12 Comparison of time co-incident values for a) valve angle and tank water level, b) valve angle and pressure at the base of the TS and c) pressure at the base of the TS and free-surface elevation at WG_01.

5 CONCLUSIONS

This paper presents the generation of tsunami scale crest only (elevated) and trough led N-waves using the 2nd generation Tsunami Simulator (TS). The elevated wave periods range from 20 to 160s and amplitudes up to 0.089m (model). The trough led N-wave periods range from 20 to 240s and in amplitude from 0.033 to 0.075m (model). The influence of flume length on the generated waves is investigated, focussing on the presence of (re-)reflection, both natural from the bathymetry and artificial from the TS, and the natural seiching within the flume.

For waves with periods less than 40s (re-)reflections do not affect the wave generation. The (re-)reflections have an influence on the position chosen for the wave calibration for waves with periods between 40 and about 120s, but do not appear to have adversely affected the wave generation. This is likely to be due to manual correction for the presence of re-reflections from the TS in the generation of waves with a longer wave length than will fit into the flume. Options for an active absorption system were explored, and suggest that a pressure transducer located at the base of the back wall of the TS is the most likely instrument to base a PID control system on. For waves significantly longer than the flume, such as the 240s N-wave, the variation in surface elevation along the flume at any instant in time is small, so the position in the flume chosen for the calibration is less critical.

Further investigation into the influence of flume length on the waves generated using the second generation TS will be conducted as part of the second phase of URBAWAVES testing, both physically and using numerical models. The use of numerical models will allow detailed investigation of the velocity field that is difficult to achieve in physical experiments. The active absorption system will also be implemented to reduce the artificial re-reflections from the TS.

ACKNOWLEDGEMENT

The authors acknowledge European Research Council (ERC) funding for the URBANWAVES project (Grant No. 336084). We acknowledge support of numerous staff at HR Wallingford, particularly Dr S Richardson, Mr O Harris and Mr I Payne, and of UCL (senior partners on the URBANWAVES grant), especially Prof T Rossetto. The authors would also like to thank the reviewer for their constructive feedback on ways to improve this paper.

REFERENCES

- Allsop, W., Chandler, I., & Zaccaria, M., 2014a. Improvements in the Physical Modelling of Tsunamis and their Effects. *Proceeding of the 5th International Conference on Application of Physical Modelling to Port and Coastal Protection, Coastlab14*, Varna, Bulgaria, 29 Sept – 2nd Oct.
- Allsop, W., Chandler, I., & Zaccaria, M., 2014b, Improving the generation of tsunami waves in physical modelling, *HR Wallingford report DDS0336-RT001*, HR Wallingford for HYDRALAB IV
- Allsop, W., Robinson, D, Charvet I, Rossetto, T. & Abernethy, R, 2008, A unique tsunami generator for physical modelling of violent flows and their impact, *Proc. 14th World Conference on Earthquake Engineering*, October, Beijing.
- Charvet I., 2011, Experimental modelling of long elevated and depressed waves using a new pneumatic wave generator, *PhD thesis*, University College London
- Charvet, I., Eames, I., & Rossetto, T., 2013. New tsunami runup relationships based on long wave experiments. *Ocean Modelling*, 69, 79-92.
- Goseberg, N., Wurpts, A. & Schlurmann, T., 2013, Laboratory-scale generation of tsunami and long waves, *Coastal Engineering*, 79, 57-74.
- Hammack, J. L., 1972, Tsunamis - a model of their generation and propagation, Rep. KH-R-28, *W. M. Keck Lab. of Hydraulics and Water Resources*, California Inst. of Technol., Pasadena
- HR Wallingford, 2013, HR DAQ - Data acquisition and analysis software programme, *HR Wallingford report AAK2150-RT008-R01-00*, HR Wallingford, UK
- Kajitani Y., Chang, S. E., & Tatano, H., 2013. Economic impacts of the 2011 Tohoku-Oki earthquake and tsunami. *Earthquake Spectra*, 29, S1, 457-478.
- Kim, Y. C., 2010, *Handbook of coastal and ocean engineering*, World Scientific Publishing Co. Pte. Ltd., Singapore, ISBN-13 978-981-281-929-1
- Madsen PA, Fuhrman DR, & Schäffer HA., 2008, On the Solitary Wave paradigm for Tsunamis, *Jo. Geophys. Research*, 113:C12012.
- McGovern, D. J, Chandler, I. & Rossetto, T., 2016, Experimental study of the runup of tsunami waves on a smooth sloping beach, *Proceeding of the 6th International Conference on Application of Physical Modelling to Port and Coastal Protection, Coastlab16*, Ottawa, Canada, 10-13 May.
- Rossetto, T., Allsop, W., Charvet, I. & Robinson, D., 2011, Physical modelling of tsunami using a new pneumatic wave generator, *Coastal Engineering*, 58(6), pp. 517-527.
- Schimmels, S., Sriram, V., Didenkulova, I., & Fernandez, H., 2014. On the generation of tsunami in a large scale wave flume. *Coastal Engineering Proceedings*, 1(34), currents. 14.
- Tadepalli, S. & Synolakis, C. E., 1994, The Run-Up of N-Waves on Sloping Beaches, *Proceedings of the Royal Society A*, 445(1923), 8 April, pp. 99-112.
- Wilkie M. J. & Young G. A. J., 1952, Pneumatic Tide Generator, *The Engineer*, July 1952